

Ultrasonic Velocity and Dispersion in Liquid Helium II from 0.15 to 1.8°K*

W. M. WHITNEY

Jet Propulsion Laboratory, California Institute of Technology, Pasadena, California

AND

C. E. CHASE

National Magnet Laboratory, Massachusetts Institute of Technology, Cambridge, Massachusetts

(Received 11 January 1967)

From the measurement of changes in the delay experienced by an ultrasonic pulse traversing a fixed path, the temperature dependence of the velocity of sound in liquid helium under its saturated vapor pressure has been determined from 0.15 to 1.8°K at the frequencies 1.00, 3.91, and 11.9 Mc/sec. A phase-comparison technique made it possible to resolve velocity changes amounting to a few mm/sec. With increasing temperature, the velocity u_1 increases above its asymptotic limit u_{10} at 0°K, passes through a maximum near 0.7°K, and decreases rapidly at higher temperatures. The velocity difference over any temperature interval that extends from below 0.2 to above 1.1°K is independent of frequency, but within the temperature range indicated u_1 increases with frequency and the position of its maximum shifts to higher temperatures. At (1.00, 3.91, 11.9) Mc/sec the maximum velocity lies (5, 7, 14) cm/sec above u_{10} and occurs at (0.65, 0.70, 0.72)°K. The dispersion is greatest in the neighborhood of 0.9°K, where the attenuation coefficient goes through a maximum. Within experimental error, the theory of Khalatnikov and Chernikova accounts for the separation between the velocity-versus-temperature curves at the three frequencies. Combination of the velocity changes measured in these experiments with values of the absolute velocity obtained by other workers above 1°K yields $u_{10} = 238.3_0 \pm 0.1_3$ m/sec.

I. INTRODUCTION

ALTHOUGH there have been many experimental studies of the propagation of ordinary sound in liquid helium below 1°K, it is the absorption that has received most of the attention, and the behavior of the velocity u_1 at these temperatures is not precisely known. The measurements of Van Itterbeek, Forrez, and Teirlinck,^{1,2} made at several frequencies in the range 200–1500 kc/sec, are accurate to within $\pm 0.1\%$, but cover only the limited temperature range 0.985–1.15°K. The values for u_1 in liquid ⁴He obtained at 5 Mc/sec by Laquer, Sydoriak, and Roberts³ in the course of their investigations with liquid ³He have errors estimated to be less than $\pm 0.2\%$, but the lowest point lies at 0.92°K. Two sets of measurements in which lower temperatures were achieved are far less accurate than those already

mentioned. Chase and Herlin⁴ determined u_1 from pulse-delay measurements at 12 Mc/sec at 0.1°K and above. Values of the velocity at temperatures as low as 0.05°K have been derived by Keen, Matthews, and Wilks⁵ from acoustic impedance measurements at 1000 Mc/sec. In both of these experiments, changes in velocity amounting to less than 2–3% could not have been resolved.

Our objectives in the research described herein were to ascertain the temperature and frequency dependence of the velocity u_1 in liquid ⁴He under its saturated vapor pressure at temperatures below 1°K, and in particular to look for dispersion near 0.9°K, where the attenuation coefficient goes through a maximum.⁴ By using the phase-comparison technique previously employed in a study of the velocity near the lambda point,⁶ with which changes in u_1 amounting to five parts per million can be resolved, we have been able to observe and measure effects lying well within the limits of error of the measurements cited above.

The temperature variation of the velocity at 1.00 Mc/sec has been described in a preliminary report.⁷ It was found that, with increasing temperature, the velocity u_1 at first increases above its low-temperature limit u_{10} , reaches a maximum value that lies approximately 5 cm/sec above u_{10} near 0.65°K, and falls rapidly at higher temperatures. In this paper we give a detailed account of that experiment, and present

*The experiments to be described were performed by the authors in the Department of Physics at Massachusetts Institute of Technology. Support for the work was provided in part by the Advanced Research Projects Agency under Contract No. SD-90, in part by the National Science Foundation, and in part (through Lincoln Laboratory) by the U. S. Air Force. The analysis of the results and the preparation of this paper have been carried on largely at the authors' present institutions. For these concluding portions of the research, we acknowledge assistance received from the Jet Propulsion Laboratory, supported by the National Aeronautics and Space Administration under Contract No. NAS 7-100, and from the National Magnet Laboratory, supported by the U. S. Air Force Office of Scientific Research. Preliminary accounts of these experiments have been given at meetings of the American Physical Society [*Bull. Am. Phys. Soc.* **7**, 472 (1962); **7**, 621 (1962)], and in Ref. 7.

¹ A. Van Itterbeek, G. Forrez, and M. Teirlinck, *Physica* **23**, 63 (1957).

² A. Van Itterbeek, G. Forrez, and M. Teirlinck, *Physica* **23**, 905 (1957).

³ H. L. Laquer, S. G. Sydoriak, and T. R. Roberts, *Phys. Rev.* **113**, 417 (1959).

⁴ C. E. Chase and M. A. Herlin, *Phys. Rev.* **97**, 1447 (1955).

⁵ B. E. Keen, P. W. Matthews, and J. Wilks, *Proc. Roy. Soc. (London)* **A284**, 125 (1965).

⁶ C. E. Chase, *Phys. Fluids* **1**, 193 (1958).

⁷ W. M. Whitney and C. E. Chase, *Phys. Rev. Letters* **9**, 243 (1962).

additional data obtained from similar measurements at 3.91 and 11.9 Mc/sec from 0.15–1.8°K. The new results show that the change in velocity Δu_1 over any temperature interval that spans the region 0.2–1.1°K is the same at all three frequencies, within experimental error, but the velocity shows a clear variation with frequency at intermediate temperatures. At 11.9 Mc/sec, for example, the peak velocity occurs near 0.72°K and lies 14 cm/sec above u_{10} . The dispersion is greatest on the high-temperature side of the velocity maxima: At 0.9°K the velocity difference over the frequency interval 1.00–11.9 Mc/sec reaches 20 cm/sec.

The behavior of the sound velocity at low temperatures has been studied theoretically by Andreev and Khalatnikov.⁸ They found that u_1 should initially rise above u_{10} as the temperature increases from 0°K, as we had observed, but their calculations were made for infinite frequency, and numerical values of the difference $u_1 - u_{10}$ obtained from their final expression did not agree closely with our 1-Mc/sec results. Recently, Khalatnikov and Chernikova have published a more comprehensive theory of sound propagation in liquid helium,^{9,10} and have demonstrated that their equations give a good account of existing attenuation data over a wide temperature range, including the low-temperature side of the absorption peak.¹¹ We will show that, within the accuracy of the measurements, the new theory also describes the dispersion observed in our experiment. Our results are also compatible with the predictions of the three-phonon theory of Pethick and ter Haar¹²; however, this agreement merely reflects the fact that the expressions for the absorption coefficient α_1 and for the velocity difference $\delta u_1(\omega, T) \equiv u_1(\omega, T) - u_1(0, T)$ that come out of the two different approaches are almost identical in the limit of high frequency and low temperature.

We include in the paper a description of the method whereby the velocity differences measured in our experiment are combined with values of u_1 obtained above 1°K by other workers to give $u_{10} = 238.30 \pm 0.13$ m/sec for the asymptotic limit of u_1 at $T = 0^\circ\text{K}$.

II. EXPERIMENTAL METHOD

Temperatures below 1°K were reached by adiabatic demagnetization. The sound chamber is imbedded in a matrix of tightly packed crystals of the paramagnetic salt (iron ammonium alum) that serves both as coolant

and thermometer. Liquid helium fills the interstices of the compacted salt mass and the interior of the chamber. Since the demagnetization cryostat in which the salt and the sound etalon are contained has been described in a recent publication,¹³ we can forego further comment here, and concentrate on the method used to measure small changes in the sound velocity. This technique has been described in Ref. 6, but a somewhat more complete account is necessary to prepare the way for a discussion of errors.

Sound waves are excited and received by two X-cut quartz crystals, each 1 cm in diam., closely matched in resonant frequency, backed with conical brass electrodes to reduce ringing and mounted with their faces accurately parallel. An ultrasonic pulse produced by one crystal traverses the distance d to the other in time $t(T) = d/u_1(T)$ at temperature T . We do not measure the total time t , and thus our experiment does not yield the absolute value of the velocity u_1 . Instead, we determine the variation in transit time $\Delta t(T, T_0) = t(T) - t(T_0)$ that accompanies a change in temperature from T_0 to T . If, from an independent experiment, the velocity is known at one temperature T_0 , its value at any other will be

$$u_1(T) = u_1(T_0) \{1 + u_1(T_0) \Delta t(T, T_0) / d\}^{-1}. \quad (1)$$

The apparatus with which the time increments Δt are measured is shown schematically in Fig. 1. A continuously running oscillator, controlled by a quartz crystal whose resonant frequency is approximately

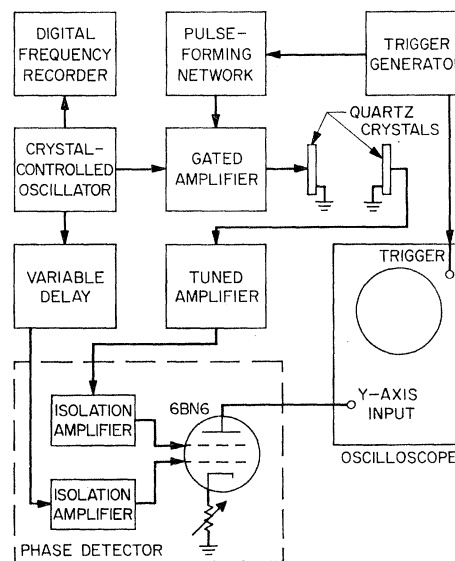


FIG. 1. Schematic diagram of electronic apparatus used for the measurement of delay. The ultrasonic etalon containing the quartz crystals is immersed in liquid helium. The variable resistor in the cathode circuit of the 6BN6 is used to establish the proper operating point for the tube.

⁸ A. Andreev and I. Khalatnikov, Zh. Eksperim. i Teor. Fiz. 44, 2058 (1963) [English transl.: Soviet Phys.—JETP 17, 1384 (1963)].

⁹ I. M. Khalatnikov and D. M. Chernikova, Zh. Eksperim. i Teor. Fiz. 49, 1957 (1965) [English transl.: Soviet Phys.—JETP 22, 1336 (1966)].

¹⁰ I. M. Khalatnikov and D. M. Chernikova, Zh. Eksperim. i Teor. Fiz. 50, 411 (1966) [English transl.: Soviet Phys.—JETP 23, 274 (1966)].

¹¹ I. M. Khalatnikov and D. M. Chernikova, JETP Pis'ma v Redaktsiyu 2, 566 (1965) [English transl.: JETP Letters 2, 351 (1965)].

¹² C. J. Pethick and D. ter Haar, Physica 32, 1905 (1966).

¹³ W. A. Jeffers, Jr., and W. M. Whitney, Phys. Rev. 139, 1082 (1965).

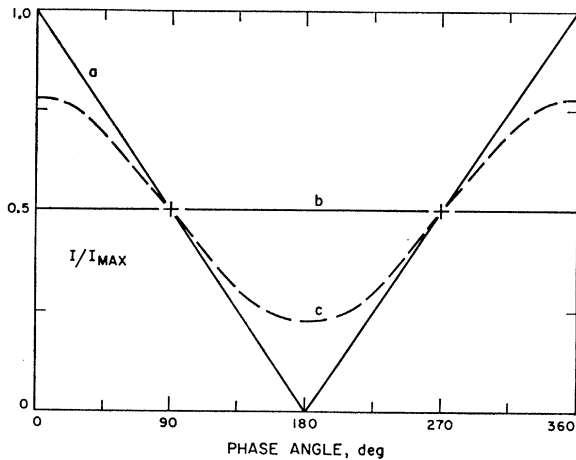


FIG. 2. Current versus phase characteristics for the phase detector (idealized). Curves (a), (b), and (c) correspond to signal amplitudes much greater than, much smaller than (i.e., zero), or comparable with, the voltage required to saturate the plate current. For all three curves it is assumed that the cw reference signal produces saturation, and that the grid bias voltage has been adjusted so that the quiescent plate current is $I_{\max}/2$. The crosses designate the optimum operating points.

equal to that of the ultrasonic crystals (when the latter are immersed in liquid helium) serves as a stable frequency standard and phase reference—that is, as a clock. Pulses of the sinusoidal signal from the oscillator are produced with a gated amplifier to drive the transmitting crystal. The delayed signal generated at the receiving crystal is amplified and led to a phase detector, where its phase is compared with that of the clock.

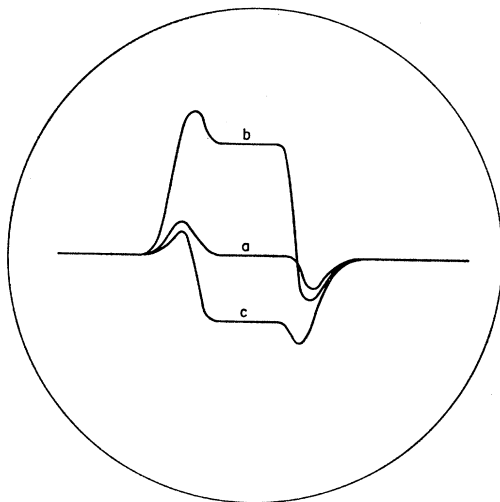


FIG. 3. Three oscilloscope traces of the signal obtained from the phase detector in the vicinity of the received pulse, shown superposed and idealized. Curve (a) illustrates the criterion used for a null—the vertical deflection of the flat portion is zero with respect to the undeflected trace. Curves (b) and (c) show changes in plate current resulting from equal but opposite changes in phase about an operating point. One of the two optimum operating points (Fig. 1) is established by varying the cathode resistor until the amplitudes of these deflections are equal.

The phase detector employs a 6BN6 gated-beam tube, whose use for this purpose has been discussed by Holman.¹⁴ With proper biasing of two of the control grids, the output current of the tube is saturated when the voltages of signals applied to these grids are simultaneously large and positive, and is zero when either voltage is large and negative. In principle, when the grid signals are sinusoidal and of sufficient amplitude, the average output current will vary linearly with the phase difference between the signals, as shown by the solid line in Fig. 2. In practice, to obtain an output characteristic that is highly linear over a wide range of phase angle is difficult, and it is preferable to use the detector as a null indicator. Therefore a variable delay line is inserted in the reference channel, and is adjusted to keep the phase difference ϕ_0 between the received pulse and the displaced cw reference signal constant. The value of ϕ_0 is not known exactly and need not be, but it is important that it remain constant during a series of measurements.

The output signal from the phase detector is displayed on an oscilloscope screen. Three idealized traces are shown superimposed in Fig. 3. Only in the immediate vicinity of a pulse is the sweep deflected. If the difference between the resonant frequency of the ultrasonic crystals and the driving frequency is sufficiently small, the central region of the pulse will be approximately flat, as shown in the figure. In our experiments, the variable delay is adjusted until this portion is coincident with the undeflected trace (curve a), a condition that we shall refer to as a null. What ever phase difference yields a null corresponds to the phase angle ϕ_0 defined above.

If there is sufficient difference between the resonant frequencies of the driving crystal and the ultrasonic crystals, beats are observed in the output of the phase detector,¹⁵ and it is difficult to select a suitable criterion for balance. It is possible to use z-axis modulation of the oscilloscope to mark a spot on the trace, and to define a null as that setting of the delay line for which the spot is undeflected. Unfortunately, the spot shifts in position relative to the pulse as the temperature and velocity change, and the settings of the delay line may then be systematically displaced from their true values. Such difficulties were avoided by insuring that the frequency mismatch was small in comparison with the reciprocal pulse duration.

It can be seen from Fig. 2 that, within each cycle there are two phase angles for which the null condition can be achieved. Two adjacent nulls will not be equivalent; by this we mean that equal changes in phase about such points will produce opposite changes in output current (curves b and c in Fig. 3). Furthermore they will in general not be one-half cycle apart. The phase

¹⁴ F. S. Holman, Jr., *Electronics* 26, 180 (1953).

¹⁵ We do not understand specifically how these beats are produced; presumably they arise from nonlinear coupling among the various complex modes of the ultrasonic transducers.

difference between two equivalent nulls is of course exactly one cycle or an integral multiple thereof. For measurement of arbitrarily large delay increments, it is desirable that the variable delay be adjustable over one full cycle, so that as one null moves out of range, the operating point can be switched to another one that is equivalent.

The transition from zero to saturation current in the 6BN6 takes place within a rather narrow range of grid voltage, and the value of φ_0 thus depends strongly upon the bias conditions for the grids. It is possible to adjust their voltages, for example by varying a resistor in the cathode circuit¹⁴ (see Fig. 1), so that curve a in Fig. 3 corresponds to $\varphi_0=90^\circ$ or $\varphi_0=270^\circ$. These two operating points are indicated by crosses in Fig. 2. When they are used, the output of the phase detector is least sensitive to small changes in amplitude of the input signal. This advantage is an important one. The errors that result from amplitude changes and the manner in which the optimum operating point was established will be discussed in Sec. IV.

At the phase detector, the received pulse will differ in phase from the cw reference signal by an amount

$$\varphi = 2\pi f\{t(T) - \tau\} + \epsilon - 2\pi n, \quad (2)$$

where f is the oscillator frequency, τ is the delay introduced by the delay line, ϵ is a temperature-independent phase shift originating within the electrical apparatus, and n is an integer—for convenience, the one for which $0 \leq \varphi \leq 2\pi$. To the extent that φ , f , and ϵ are independent of time, changes in the transit time $t(T)$ are directly observed as changes in τ . The variable delay lines used in our experiments can be set to any value up to the maximum with a reproducibility of better than one part in a thousand by means of an attached multiturn dial. In the apparatus used at 1 Mc/sec, the maximum delay is 1 μ sec and the sensitivity of the phase detector is such that a change in delay of approximately 1 nsec produces a deflection on the oscilloscope screen that is distinguishable from noise. The corresponding relative change in velocity is $\delta u_1/u_1 = \delta\tau/t(T) = u_1\delta\tau/d$. Using $d = 5$ cm, $u_1 = 2.4 \times 10^4$ cm/sec, we obtain $\delta u_1/u_1 \sim 5 \times 10^{-6}$. Velocity changes of approximately 1 mm/sec can thus be resolved; however, because of certain systematic errors, to be discussed below, measured delays that are comparable with a full period of the reference signal can be in error by several percent.¹⁶

¹⁶ The sensitive response of the phase detector to small velocity changes enables us to observe an interesting property of the Ashmead conical valve that is used to isolate the internal chamber of the demagnetization cryostat from the external helium bath (see Refs. 4 and 13.) The seating of the upper cone into the lower one is accompanied by a momentary change in the output of the phase detector, in a direction that signifies an increase in velocity. The more rapidly the cone is pushed into place, the greater the deflection. We attribute this effect to compression of the liquid helium within the inner can by the descending cone. The short duration of the phase excursion indicates that, although the valve effectively blocks the flow of normal fluid and thereby inhibits the

III. DATA REDUCTION

The settings of the delay line τ [see Eq. (2)] and their corresponding temperatures constitute the primary data in the experiment. Several steps are required to convert these numbers to values of the velocity $u_1(T)$. For the sake of presenting a coherent account of them, we briefly describe the entire process here, leaving an elaboration of some of the details for a later section.

It is the changes in τ that are of interest to us rather than their absolute values, and for convenience we specify delay settings for each demagnetization with respect to their extrapolated value at $T=0^\circ\text{K}$. The adjustment is carried out by a process similar to that used in a previous analysis of attenuation data.¹³ It is assumed that, for temperatures below some upper limit T_{max} , the temperature variation of τ can be described by the empirical relation

$$\tau = AT^n + B. \quad (3)$$

For reasons given later, we choose $n=3$, $T_{\text{max}}=0.5^\circ\text{K}$. The constants A and B for each demagnetization are determined by a least-squares fit to all the values of τ for which $T \leq T_{\text{max}}$. We compute the difference $\tau - B$ for each experimental point, convert it from units of divisions on the delay dial to nanoseconds, using a predetermined calibration factor for the delay line, and divide it by the crystal spacing to obtain what we shall call the reduced delay τ_r . In the subsequent analysis it is easier to work with smoothed values of τ_r than with the numerous individual data points (of which there were more than 2000). The region of temperature covered in the measurements is therefore divided into fields 0.1 K° wide. Values of τ_r from all demagnetizations at a given frequency are combined, and a least-squares determination is made of the third-degree polynomial that best fits the points within each field, with the requirement that the slope and value of the curve be continuous from one field to the next. We emerge from these calculations with an empirical function $\tau_r(T)$ representing the change in the time required for an ultrasonic pulse to travel one cm when the temperature changes from 0°K to T .

The temperature 0°K serves as a natural reference point for the velocity as well as for the reduced delay. Equation (1) as it stands relates the velocity at temperature T to a known velocity at a reference point T_0 and to a delay measurement over the interval from T_0 to T . We use this expression in reverse to determine the limiting velocity at 0°K . In terms of the velocity and the reduced delay, both at temperature T ,

$$u_{10} = u_1 / (1 - u_1 \tau_r).$$

This relation can be interpreted as a mapping of known velocities at different temperatures into the single

transfer of heat from the bath to the inner can, it presents little obstruction to the flow of superfluid, and pressure equilibrium is rapidly established.

point u_{10} . Although the empirical function τ_r through which the projection is accomplished is known only to within a few percent, the final uncertainty in u_{10} is largely a reflection of errors in u_1 . From a study of all the values of u_{10} derived from a given set of velocity measurements at different temperatures, we can draw conclusions about the reliability of the original data and can compare the results of one experiment with those of another. By combining the results of several experiments, we obtain a "best" value for u_{10} whose reliability somewhat exceeds that of any one of the contributing terms.

When u_{10} is known, smoothed values of the velocity and of the velocity difference $u_1 - u_{10} = -u_{10}^2 \tau_r / (1 + u_{10} \tau_r)$ are calculated as a function of temperature; these numbers represent our final results.

IV. ERRORS

The most interesting effects revealed by our measurements represent very small changes in delay, so we must consider rather carefully what errors might be present in the final results. According to Eq. (1), we should be concerned with the uncertainty in the reference velocity and with the errors arising in the measurement of the crystal spacing, the temperature, and the incremental delay Δt . As mentioned in the preceding section, 0°K is the reference temperature T_0 . The error brought in with u_{10} is approximately 0.1 m/sec (see Sec. V). This uncertainty largely determines the errors in the values of u_1 computed from Eq. (1), but nonetheless it is small enough so that it does not add appreciably to errors from other sources in the velocity differences $\Delta u_{10} = u_1 - u_{10}$, and in particular it does not affect the temperature dependence of Δu_{10} . To compute the crystal spacing d at liquid-helium temperatures, we subtract 0.4%¹⁷ from the separation measured at room temperature to allow for thermal contraction of the brass sound chamber. The path lengths thus obtained are estimated to be correct to ± 0.002 cm, so that only for the very short spacings used at 12 Mc/sec will errors from this source be as large as 1%. Errors in Δt arising from changes in the crystal spacing as the etalon warms up after a demagnetization are entirely negligible, amounting to less than 1% of the smallest time interval that can be resolved with the phase detector. Consequently, the accuracy of our final values of Δu_{10} is restricted primarily by errors in the measurement of temperature and delay.

1. Errors in Temperature Measurement

The temperature of the liquid helium in the sound chamber is derived from measurements of the mutual

inductance of a coil centered on the paramagnetic salt crystals, as in Ref. 13. Except at the very lowest temperatures (below 0.3°K for iron-ammonium alum), temperatures and mutual-inductance readings are related by the expression $M = M_0 + A/(T - \Delta)$, where Δ is an effective Curie-Weiss constant for the salt pill (including a geometrical correction), and A and M_0 are constants determined by calibrating the thermometer against the vapor pressure of liquid helium above approximately 1.3°K. It is found by repeating the calibration periodically that, although A remains constant during a run, M_0 slowly changes. This effect was observed during the attenuation measurements reported in Ref. 13, and was attributed there to instability of the oscillator that drives the Hartshorn bridge. When we substituted a highly stable 33½ cps source for the audio oscillator used before, however, we found that the drift was reduced but still not completely eliminated, so our previous explanation must be considered incomplete.

The changes in M_0 observed during our runs would cause rather large errors in Δu_{10} if we did not correct for them. When the temperature derived from an inductance reading differs from the true temperature by an amount $\delta_e T$, the error in the velocity difference $u_1(T_2) - u_1(T_1)$ will be approximately $(\partial u_1 / \partial T_2) \delta_e T_2$ if T_1 lies in the region below 0.7°K over which $\partial u_1 / \partial T \sim 0$. From 0.9°K on up to the lambda point, the derivative increases steadily in absolute value as the temperature increases. At 1.6°K, where $|\partial u_1 / \partial T| \sim 12$ m/sec K°, a 2% error in T leads to a systematic error of approximately 10% in Δu_{10} .

To compensate for the drift in the thermometer characteristics, we took several calibration points after the apparatus had warmed up to bath temperature. The value of M_0 calculated from these, rather than from points taken just before demagnetization, was used in computing temperatures from all the inductance readings made during the warmup period. By this procedure we use an erroneous value of M_0 at low temperatures rather than high. Here the relative errors in temperature $\delta_e T / T$ are small because $M - M_0$ is large, and their influence on Δu_{10} is reduced by the weak temperature dependence of u_1 . We estimate that temperature errors above 1°K are held to within a few millidegrees, and the error from temperature uncertainty in Δu_{10} at 1.6°K, to complete the example given above, is 1% rather than 10%.

As before,¹⁸ a small correction is made for the position of the movable cone in converting mutual inductance readings to temperatures.

2. Errors in Delay Measurement

We rewrite Eq. (2) to indicate how experimental parameters other than temperature influence the delay

¹⁷ R. J. Corruccini and J. J. Gniewek, (U. S.) Natl. Bur. Std. (1961), Monograph 29, p. 9.

measurement:

$$\tau = t(T) - n/f(t') + [\epsilon(t', \tau) + \varphi(t', A)]/2\pi f(t'), \quad (4)$$

where t' denotes time during a run (not delay), and A is the amplitude of the received pulse at the phase detector. Guided by this relationship, we assign errors in the values of reduced delay τ_r derived from the delay settings τ to the five sources discussed below.

(a) *Drift in the Oscillator Frequency*

An accurate measurement requires, to begin with, a stable clock. It follows from Eq. (4) that a frequency change δf will produce a phase difference $\delta\varphi = 2\pi\delta f(t - \tau) \sim 2\pi d\delta f/u_1$ (since $t \gg \tau$) between the received pulse and the reference signal, requiring that the variable delay be adjusted by an amount $\delta\tau \gg (\delta f/f)d/u_1$ to restore balance. For all of our demagnetizations, with the exception of three at 12 Mc/sec, the reference oscillator was crystal controlled, and the frequency drift during a run amounted to no more than a few cycles per second. The corresponding total shift in delay is somewhat too small to be resolved with the phase detector. During our 12-Mc/sec measurements at a path length of 0.51 cm, the frequency of the control crystal was not sufficiently close to the resonant frequency of the ultrasonic crystals, and it was necessary to use a signal generator as a clock. The frequency drifted by several parts in 10^4 during the warmup period following demagnetization, with a corresponding change in delay $\delta\tau \leq 10$ nsec. During each phase measurement, the frequency was read from the digital frequency recorder and a correction was made.

(b) *Electrical Instabilities*

Drifting of the electrical phase shift ϵ or of the operating point φ of the 6BN6 will lead to variations in the output of the phase detector that are unrelated to changes in the transit time of the ultrasonic pulse. That such effects were absent in our experiments is shown indirectly by the fact that the phase readings at a given temperature were the same before and after each run, within the limits imposed by temperature uncertainties. To look directly for instabilities, we fed the transmitter signal through an attenuator to the amplifier and phase detector, and during a series of measurements we alternately compared both this signal, which suffered only an electronic delay, and the ultrasonic signal with the clock. Small systematic displacements of the phase of the transmitted signal were occasionally observed, but they produced no significant changes in the final results when corrections were made for them. We believe that any errors from this source in our experiment are small in comparison with those yet to be discussed.

(c) *Nonlinearities in the Delay Line*

The variable delay is calibrated by finding all positions of the multiturn dial which yield equivalent

nulls. Since the frequency of the reference signal can be measured to within 0.1 cps with the digital frequency recorder, the period of the clock is very accurately known, and the average delay corresponding to one division on the delay dial can be calculated. However, the amount by which the phase of the reference signal is shifted by the variable delay is not exactly proportional to the dial setting, as we have indicated in Eq. (4) by representing the phase angle ϵ as a function of τ . Two different variable delays were used in the measurements: a 1- μ sec line at both 1 and 4 Mc/sec, and a 0.25- μ sec line at 12 Mc/sec. According to the specifications for these units, a fractional increase in dial setting is accompanied by the same fractional increase in delay to within $\pm 2\%$. Measurements of delay differences amounting to less than one cycle are therefore uncertain by this amount, but since whole-cycle portions of each delay line can be calibrated against the clock, the error from nonlinearity is of course much less than 2% for measured time intervals longer than one period.

If the delay line is not properly matched in impedance with the circuit in which it is incorporated, a standing wave is set up in it, and the reference signal picked up by the slider as it moves along the line is sinusoidally displaced in phase from what would be observed if delay were strictly proportional to dial setting. Such a periodic phase error introduces a second type of nonlinearity in the delay line. Although the amplitude of these phase oscillations can be minimized by careful adjustment of the resistances with which the line is terminated, it cannot be reduced to zero.

With a standing wave present in the delay line, the temperature dependence of the settings of the delay dial required for balance of the phase detector is given by the equation

$$\tau(T) - \tau(0) = d\tau_r(T) + S \sin\{4\pi d f \tau_r(T) + \delta\} - S \sin\delta, \quad (5)$$

where $\tau_r(T)$ is the true reduced ultrasonic delay defined previously. The phase factor δ , whose value is in general not known, depends upon the position of the slider at $T = 0^\circ\text{K}$. The amplitude S of the phase oscillations was determined by measuring the standing wave ratio at the slider terminal. The magnitude of S sets an upper limit to the error in the delay $\delta_\epsilon\tau = \tau(T) - \tau(0) - d\tau_r(T)$.

It is important to realize that the amplitude of the error in the reduced delay $\delta_\epsilon\tau/d$, and thus also in the velocity difference Δu_{10} , depends upon the ratio S/d . Since S is a characteristic of the delay line and its associated elements, the error in τ_r , for a given phase detector, increases as the crystal separation decreases. From a study carried out at 4 Mc/sec with the phase detector which incorporated the 1- μ sec line, we found $S = 7$ nsec. The expected amplitude of the oscillations in τ_r would be 3.5 nsec/cm for the results at 4 Mc/sec ($d \sim 2$ cm), and 1.4 nsec/cm at 1 Mc/sec ($d \sim 5$ cm). For

the apparatus used with the 0.25- μ sec delay line, $S=1.8$ nsec. The amplitudes of the errors in τ_r at 12 Mc/sec for the crystal spacings 0.256, 0.386, and 0.51 cm would thus be 7, 4.7, and 3.5 nsec/cm, respectively. Because these errors are periodic in delay rather than cumulative, their effect on the results is most noticeable at temperatures for which the sine term in Eq. (5) goes through its first maximum, i.e., where τ_r and the magnitude of its slope $|d\tau_r/dT|$ are both relatively small. At higher temperatures, where $|d\tau_r/dT|$ is large, random temperature errors mask the systematic phase deviations.

(d) *Amplitude Sensitivity of the Phase Detector*

The current versus phase characteristic of the 6BN6 depends to some extent upon the magnitudes of the voltages applied to the two control grids. Changes in the amplitude of the reference signal or of the signal obtained from the ultrasonic receiving crystal will therefore produce spurious indications of a phase change in the phase detector. The reference voltage, which may vary with the setting of the variable delay because of standing waves and losses in the delay line, can always be made large enough so that the phase detector is saturated for all positions of the slider, and we believe that errors from this source can be ignored. The amplitude of the received ultrasonic pulse, however, depends upon the attenuation of sound in liquid helium, which changes by more than an order of magnitude over the temperature range covered in our experiments. If the crystal spacing is too great, the signal vanishes into noise at temperatures for which the attenuation is large. At the cost of reduced resolution in the velocity measurement, the path length is made small enough so that the signal voltage changes by no more than a factor of three during a series of measurements.

Further steps to reduce the errors from amplitude changes are dictated by the characteristics of the phase detector. The relationship between the instantaneous current i_p and the voltages E_1 and E_3 on grids 1 and 3 of the 6BN6 can be represented quite well by the empirical equation

$$i_p = (I_{sat}/4)\{1 + \tanh E_1\}\{1 + \tanh E_3\},$$

where $E_1 = B + A \sin \omega t$ and $E_3 = B + C \sin(\omega t + \varphi)$. The amplitudes of the received pulse and the reference signal are A and C , respectively. The dc grid bias B is the same for both grids; as stated earlier, its value is adjusted by means of a single cathode resistor (Fig. 1). The voltage to which B is referred is that for which the quiescent dc plate current is $I_{sat}/4$.

The output characteristics of the phase detector can be derived from the phase and amplitude dependence of the time-averaged value of i_p . The effect of amplitude changes on the current-phase relationship is indicated schematically by the three curves in Fig. 2, for all of which $B=0$. The solid V-shaped curve (a) represents the ideal characteristic discussed earlier, corresponding to large values of both A and C . Curve (b), for which

the current has the constant value $I_{max}/2$, corresponds to $A=0$. The dashed curve (c) represents a typical characteristic for moderately large A and large or moderately large C . For $B=0$, the output current is independent of amplitude when $\varphi = \pm\pi/2$, so these values define the most satisfactory operating points. For $B \neq 0$, curves (b) and (c), but not curve (a), will be shifted upward or downward, and the phase-detector output will respond to changes in amplitude even when $\varphi = \pm\pi/2$.

The above discussion shows how important it is to find the proper operating point for the phase detector before actual measurements begin. The criterion for a null (see Fig. 3) is that the output of the phase detector be the same when there is a pulse ($A \neq 0$) as when there is not ($A=0$). To establish an operating point, we adjust the variable delay to obtain a null, for which the phase difference will be approximately 90° or 270° . The bias voltage B is then adjusted until equal changes in delay about the null yield equal but opposite changes in output. Following this step, the bias voltage will still be slightly above or below the optimum value, and some amplitude dependence will remain. To determine the magnitude of such residual effects, we apply a pulse through an attenuator to the grid of the 6BN6 and adjust the pulse amplitude over a wide region that includes the voltages anticipated during the run. It is found that there is a certain range of voltages over which the phase-detector output exhibits its weakest amplitude dependence. Prior to a demagnetization, transmitter voltages and amplifier settings are chosen so that, if possible, the pulse voltages at the grid of the 6BN6 will lie within this range during the measurements.

The errors from amplitude sensitivity are greatest at temperatures just above the region of the velocity maximum, where the attenuation of sound reaches its peak values. Even at the smallest signal levels, the signal-to-noise characteristics of the components used at 1 Mc/sec were such that the output pulse saturated the phase detector. Before each run, we were therefore able to adjust the amplitude of the received pulse (by varying the gain of the amplifier) to the level for which the amplitude sensitivity would be minimum. We believe that by this step we held systematic errors in τ_r from amplitude effects well below an estimated maximum value of 3 nsec/cm. From a study carried out at the conclusion of the run at 4 Mc/sec, we ascertained that amplitude errors in τ_r in these measurements would have been less than 5 nsec/cm. The maximum errors in the reduced delay at 12 Mc/sec are estimated to be 4 nsec/cm or less.¹⁸

¹⁸ In the apparatus designed by R. J. Blume [Rev. Sci. Instr. 34, 1400 (1963)] for following small variations in velocity, changes in the transit time of the ultrasonic pulse are used to control the frequency of the reference oscillator so that the phase-detector output will remain constant. Changes in velocity are thus manifested directly as variations in frequency, which can be accurately measured. The errors that arise in our experiments from characteristics of the delay line are thereby avoided, although apparently some problems associated with amplitude sensitivity remain.

(e) Electrical Interference at the Receiving Crystal

We have mentioned the necessity of using a short ultrasonic path at the higher frequencies to keep the change in amplitude of the received signal within bounds, and in part (c) above we pointed out that the errors in τ_r from standing waves in the delay line grow larger for a given phase detector as the crystal spacing is made smaller. Here we mention an additional difficulty that affects the accuracy of the measurements at the shorter paths. The pulse duration must be smaller than the time required for the ultrasonic pulse to travel from transmitter to receiver, in order to minimize interference between two coherent electrical signals at the receiving crystal: one generated by the ultrasonic pulse, the other arising from the tail of the electrical pulse applied to the transmitting crystal, which is capacitively coupled to the receiver. The error produced by such interference is similar to that arising from the standing wave in the delay lines, and represents an additional factor in the nonlinear response of the setting of the delay line to changes in transit time. In our measurements at 12 Mc/sec, for which the crystal separation was 0.5 cm or less, this interference could not be avoided, and it was noticed, particularly during the runs at 0.386 and 0.256 cm, that the shape of the received pulse changed slightly as a result of the overlap as the apparatus warmed up through the region of the attenuation maximum. We estimate that, for the measurements made with these two spacings, the values of τ_r could contain systematic errors of as much as 5 nsec/cm at these temperatures.

V. RESULTS

1. Experimental Conditions

Measurements at the frequency 1.000 Mc/sec with crystals 5.05 cm apart were made following six demagnetizations carried out on three different days. The period of time required for the apparatus to warm up from the lowest temperatures reached to 0.9°K ranged from 25–50 min. We changed the amplitude of the electrical pulse applied to the transmitting crystal from 30 to 150 mV rms to look for finite amplitude effects in the liquid helium, but the results were independent of the size of the signal.

The data at 3.910 Mc/sec for a crystal spacing of 1.98 cm are derived from three demagnetizations whose warmup times were rather short—6, 11, and 12 min. On the basis of experience gained from attenuation measurements carried out with the same apparatus,¹³ we believe that the liquid helium was nevertheless close to thermal equilibrium with the paramagnetic salt at all times. Changes in the amplitude of the input pulse from 50 to 100 to 200 mV rms had no effect on the results.

Sound pulses at 12 Mc/sec were generated by exciting the 4-Mc/sec crystals on or near their third harmonic. Warmup times for the eight runs to be mentioned

ranged from 12–40 min. For one set of three demagnetizations made with crystals 0.51 cm apart, the reference signal was derived from a signal generator rather than from a crystal-controlled oscillator, as mentioned earlier. In applying corrections for an observed drift in frequency of the cw signal, we reduced all the results to 11.897 Mc/sec. One set of measurements was made with a crystal spacing of 0.256 cm at 11.7300 Mc/sec; three sets at 0.386 cm and 11.895 Mc/sec. Pulse amplitudes for these runs ranged from 0.3 to 1.1 V rms.

2. Reduced Delay versus Temperature

The procedure by which the empirical function representing $\tau_r(T)$ is derived from the settings of the delay dial and their corresponding temperature is described in Sec. III. Numerical values for τ_r , obtained by evaluating the polynomial expression at the center of each data field and at a few additional temperatures near 0.7°K, are listed by frequency in Table I. The error accompanying each number represents the (unbiased) rms deviation of all the points within the field from the smooth curve.

The method employed to reduce the data insures that the values of τ_r obtained from different demagnetizations at the same frequency will be in agreement at the lowest temperatures. The errors listed in the uppermost rows of Table I thus indicate only the precision with which the phase detector could be balanced and read. The larger errors at higher temperatures reflect the systematic effects described in Sec. IV.

Inspection of Table I reveals that the errors in the vicinity of the velocity maximum are much greater for the 12 Mc/sec results than for those at other fre-

TABLE I. Smoothed values of the reduced delay $\tau_r = u_1^{-1}(T) - u_1^{-1}(0)$, the change in ultrasonic delay per unit path length (nsec/cm) when the temperature changes from 0 to $T^\circ\text{K}$. Each error represents the unbiased rms deviation of the experimental points from the smooth curve over an interval 0.1°K wide centered on the temperature indicated.

T (°K)	$f = 1.00$ Mc/sec	$f = 3.91$ Mc/sec	$f = 11.9$ Mc/sec
0.1	0.0±0.3	0.0±0.3	0.0±0.7
0.2	-0.3±0.3	-0.3±0.2	-0.7±0.5
0.3	-1.1±0.3	-1.4±0.2	-1.6±0.5
0.4	-2.7±0.4	-2.9±0.3	-3.9±1
0.5	-5.2±0.5	-5.4±0.5	-9.3±2
0.6	-8.2±0.5	-9.4±0.3	-17 ±3
0.65	-9.0±1	-11.3±0.4	-21 ±4
0.7	-6.6±2	-12.5±0.6	-24 ±6
0.75	1.2±3	-10.2±0.8	-24 ±7
0.8	14.1±4	-3.6±2	-19 ±8
0.85	28.4±4	9.4±2	-7 ±9
0.9	42.9±4	28.0±3	8 ±9
1.0	74.8±5	67.7±4	52 ±9
1.1	114 ±8	112 ±5	105 ±9
1.2	172 ±13	164 ±9	161 ±7
1.3	234 ±5	240 ±2	237 ±8
1.4	331 ±8	349 ±6	337 ±9
1.5	471 ±8	490 ±12	476 ±7
1.6	651 ±11		660 ±15
1.7			914 ±16
1.8			1236 ±16

quencies. For none of the runs at 12 Mc/sec were we able to minimize all of the various systematic errors simultaneously, although by varying the experimental conditions we could identify their sources. Two demagnetizations were made with pulse widths differing by a factor of two, and during one run we balanced the phase detector using two different portions of the received pulse, both steps to verify that there was interference between the received pulse and its background. During two runs at 0.386 cm we measured the phase of the first echo (effective path=1.16 cm), as well as that of the first transmitted pulse. Near the 12-Mc/sec attenuation peak, the amplitude of the echo was well below the level considered optimum to avoid amplitude distortion, and the heights of the velocity maxima for these runs near 0.75°K were approximately 10 nsec/cm lower in comparison with the peak values derived from the delay measurements made for the first received pulses. Lower peak values were also encountered in runs for which the amplitude of the transmitter pulse was too low. To verify the presence of standing-wave errors, we inserted a length of cable in the reference line to produce a shift in the initial position of the slider, and observed a corresponding displacement in the "nodes" of the phase oscillation. On the basis of such experiments as these, we have concluded that the maximum and minimum values of τ_r derived from the errors listed in the last column of Table I do bracket the true values in the neighborhood of the velocity maxima. Thus, although our results at 12 Mc/sec cannot be considered entirely satisfactory in this temperature region, we feel that their inclusion in this report is warranted. At the highest temperatures covered in our measurements, the errors in τ_r from temperature uncertainties exceed those arising from standing waves and other effects. Here the values at 1 and 12 Mc/sec are of comparable accuracy, while the results at 4 Mc/sec are somewhat less reliable because they are based upon fewer data.

3. Velocity of Sound at 0°K

In determining u_{10} by the method described in Sec. III, we draw upon the velocity measurements of Chase¹⁹; Van Itterbeek and Forrez (IF)²⁰; Van den Berg, Van Itterbeek, Van Aardenne, and Herfkens (BIAH)²¹; Van Itterbeek, Forrez, and Teirlinck (IFT-1,2)^{1,2}; and Laquer, Sydoriak, and Roberts (LSR).³ The results of Atkins and Chase²² are excluded because later work by Chase showed them to be too low by 0.8%.¹⁹ Our delay measurements did not extend upward far enough into the temperature region covered by Findlay, Pitt,

TABLE II. Velocity of sound in liquid helium at 0°K calculated, from measurements above 1°K in the experiments indicated and from values of τ_r . The weight has been chosen to reflect the precision of the experiment and the number of observations.

Experiment	u_{10} (m/sec)	Weight (%)
Chase ^a	239.0 ± 0.4	3
BIAH ^b	239.0 ± 0.1 ₆	7
LSR ^c	238.0 ± 0.1 ₂	10
IF ^d	238.1 ₆ ± 0.05	40
IFT ^e	238.3 ₃ ± 0.05	40
Av. u_{10} = 238.3 ₀ ± 0.1 ₃		

^a Reference 19.

^b Reference 21.

^c Reference 3.

^d Reference 20.

^e Reference 1.

Grayson-Smith, and Wilhelm,²³ and by Pellam and Squire²⁴ in their experiments, so we are unable to use their results. Measurements made below 1.05°K are ignored; our work shows that at higher temperatures there is no significant dispersion at frequencies below 12 Mc/sec, so by restricting ourselves to this region we avoid a correction for frequency in the computation of u_{10} from u_1 . The average value of u_{10} derived from each of the five experiments considered and the weight that we have assigned it in the final average are given in Table II.

Chase measured u_1 at 2 and 12 Mc/sec, using pulse techniques and a sound etalon with variable spacing between the transmitting and receiving crystals. Twelve of his points lie in the temperature region covered in our experiment, but three of the nine measurements at 2 Mc/sec are excluded because they were made below 1°K. In the experiment of BIAH, in which an optical method based upon the Debye-Sears effect in liquid helium was used,²⁵ the velocity was measured at 1 Mc/sec at 16 temperatures in the range 1.3–1.8°K. LSR measured the time required for a pulse with a 5-Mc/sec carrier to traverse a fixed path. Only four of the experimental points lie between 1.05 and 1.8°K.

Van Itterbeek and Forrez measured the velocity at 220, 420, 512, and 800 kc/sec at temperatures above 1.1°K, using an acoustical interferometer with a variable path. Later, Van Itterbeek, Forrez, and Teirlinck extended the work to lower temperatures with the same ultrasonic apparatus. The velocities tabulated in IFT-1 represent temperatures from 1.076–1.146°K and frequencies from 220 to 1480 kc/sec. In both IF and IFT-1, the experimental error is listed with each velocity value. After modifying these to take account of the errors in our own measurements of τ_r , we have made a

¹⁹ C. E. Chase, Proc. Roy. Soc. (London) **A220**, 116 (1953).

²⁰ A. Van Itterbeek and G. Forrez, Physica **20**, 133 (1954).

²¹ G. J. Van den Berg, A. Van Itterbeek, G. M. V. Van Aardenne, and J. H. J. Herfkens, Physica **21**, 860 (1955).

²² K. R. Atkins and C. E. Chase, Proc. Phys. Soc. (London) **A64**, 826 (1951).

²³ J. C. Findlay, A. Pitt, H. Grayson Smith, and J. O. Wilhelm, Phys. Rev. **54**, 506 (1938).

²⁴ J. R. Pellam and C. F. Squire, Phys. Rev. **72**, 1245 (1947).

²⁵ A. Van Itterbeek, G. J. Van den Berg, and W. Limburg, Physica **20**, 307 (1954).

simple statistical test, using standard procedures,^{26,27} to determine whether the spread in the calculated values of u_{10} is consistent with the errors in the individual observations. The data from IF and IFT-1 were treated separately. With few exceptions, the values of u_{10} derived from all the u_1 measurements at a given frequency are statistically compatible. In both experiments, the average values of u_{10} at different frequencies are distributed over a region somewhat wider than would be predicted from their errors, but the discrepancies are comparable with the estimated absolute errors of the measurements (0.1%).

We cannot use the results reported in IFT-2 because they were obtained below 1°K, but on the basis of these measurements, IFT suggest that the values at 220 kc/sec in IFT-1 might have been 0.1% too high. Our own analysis shows that the values of u_{10} at 220 kc/sec lie on the average 0.27 m/sec above those at the other frequencies. We have therefore ignored the 220-kc/sec results of IFT-1 altogether in computing the value of u_{10} listed in Table II, and in carrying out the statistical calculations referred to above.

The weight that we assign each experiment in order to compute a final average for u_{10} is somewhat arbitrary, although we made it roughly proportional to the inverse square of the error so that it reflects the precision of the measurement and the number of observations.^{26,27} We obtain $u_{10} = 238.3_0 \pm 0.1_3$ m/sec. This result is consistent with that given in our earlier report— $u_{10} = 238.2_7 \pm 0.1$ m/sec, which was based upon a reference velocity $u_1 = 234.6_1$ m/sec at 1.6°K. The best previous estimate of u_{10} was 239 ± 2 m/sec, a number obtained by extra-

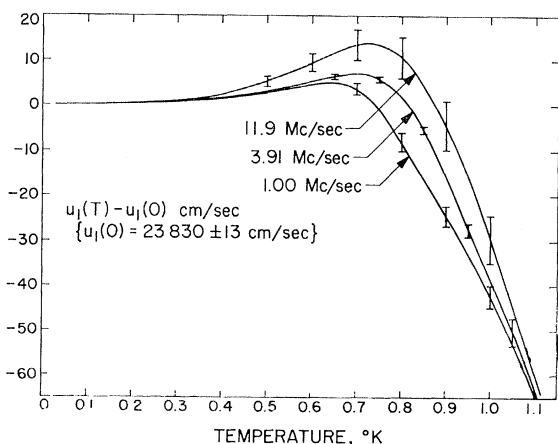


FIG. 4. Smoothed values of the velocity of sound u_1 versus temperature below 1.1°K at 1.00, 3.91, and 11.9 Mc/sec, derived from the reduced delay (Table I) with reference velocity $u_{10} = 238.30$ m/sec at 0°K. Estimated uncertainties in u_1 are indicated with vertical error bars in the region of maximum dispersion.

²⁶ R. T. Birge, Phys. Rev. 40, 207 (1932).

²⁷ David Brunt, *The Combination of Observations* (Cambridge University Press, London, 1917), especially Chap. IV.

polating measurements made at higher temperatures to absolute zero.¹⁹

4. Velocity of Sound versus Temperature

Since the number representing u_{10} has greater reliability than any single measurement of u_1 , we use it as the reference point in computing the velocity above 0°K from the reduced delay $\tau_r(T)$. The smoothed velocity difference Δu_{10} is plotted against temperature in Fig. 4 for the interval 0–1.2°K. Where the curves at the three frequencies follow different courses, we use error brackets to indicate the estimated uncertainties in Δu_{10} , which are derived from the errors in τ_r (Table I) and in u_{10} . Above 1.1°K, differences among the values of reduced delay at the three frequencies are within experimental error, so in calculating u_1 at these temperatures we combine all of the data without regard to frequency. Smoothed values of τ_r , u_1 , and Δu_{10} , calculated by the method described in Sec. III but based upon all the measurements for the temperature interval 1.1–1.8°K, are listed in Table III. Although the velocity is given to the nearest 0.01 m/sec, the uncertainty in u_{10} is 0.1 m/sec, so the numbers in the second decimal place are of significance only when velocity differences are being found. The errors in Δu_{10} in the table and in Fig. 4 are largely a reflection of those in τ_r . In our preliminary report,⁷ we gave the result $\Delta u_{10} = 3.6_6 \pm 0.1$ m/sec at 1.6°K, which had been obtained by using $u_1 = 234.6_1$ m/sec at 1.6°K as the reference velocity. This number has been changed in no significant way by the more thorough analysis to which the data have now been subjected.

Values of u_1 previously reported⁶ are shown in the final column of Table III. These were based upon measurements with the 1-Mc/sec phase detector, and their absolute values had been adjusted to give the best agreement with the velocity measurements of Van Itterbeek and Forrez.²⁰ The earlier results yield velocity differences some 8–9% smaller than our present ones for the temperature intervals 1.3–1.8°K and 1.4–1.8°K. Such discrepancies lie outside the combined

TABLE III. The reduced delay $\tau_r(T)$, the velocity $u_1(T)$, and the velocity difference $\Delta u_{10} = u_1(T) - u_{10}$ above 1.1°K, with reference velocity $u_{10} = 238.3_0 \pm 0.1_3$ m/sec. The tabulated values of τ_r were obtained by combining the experimental data at all three frequencies and smoothing them. The results in column 5 are taken from an earlier report (Ref. 6) and are to be compared with those in column 3.

T (°K)	τ_r (nsec/cm)	u_1 (m/sec)	$-\Delta u_{10}$ (m/sec)	u_1 (Ref. 6) (m/sec)
1.1	109 ± 8	237.6_8	0.62 ± 0.05	
1.2	162 ± 7	237.3_8	0.92 ± 0.04	
1.3	237 ± 7	236.9_6	1.34 ± 0.04	236.7_3
1.4	338 ± 9	236.4_0	1.90 ± 0.05	236.3_3
1.5	475 ± 9	235.6_3	2.67 ± 0.05	235.6_6
1.6	659 ± 15	234.6_2	3.68 ± 0.08	234.6_1
1.7	914 ± 16	233.2_2	5.08 ± 0.09	233.2_8
1.8	1236 ± 16	231.4_3	6.82 ± 0.09	231.7_0

errors in the measurement of delay for the two experiments, but could be accounted for if the temperatures given in Ref. 6 were 2% too low. Temperatures were derived from measurements of the vapor pressure over the liquid-helium bath while it was being pumped, and may have been in error at the lower limit of the temperature range covered in that experiment. It is worthwhile emphasizing that our present results reflect a variety of experimental conditions: three different crystal spacings, two different delay lines and phase detectors with their associated problems, and six distinct thermometer calibrations, excluding the checks made routinely at the conclusion of each series of measurements.

VI. DISCUSSION

1. Validity of Extrapolation Procedure

The presence of dispersion on the low-temperature side of the velocity maximum raises the possibility that the velocity does not obey the simple power law upon which our extrapolation of the delay measurements was based. To determine whether or not the choice of the form of Eq. (3) and of the values of the parameters n and T_{\max} had a significant influence upon the absolute values of τ_r , or upon the characteristics of the dispersion, we carried out the type of analysis that was employed in Ref. 13 to ascertain the temperature dependence of the absorption coefficient. Using all the data from a given run for which $T \leq T_{\max}$, we chose a series of values of the exponent n , and for each one determined the constants A and B and computed the sum of residuals $R_n = \sum (\tau_r - AT^n - B)^2$. A minimum in R_n at a certain value of n (denoted by n_{\min}) was taken as an indication that the fit between the data and the empirical equation was optimum. These calculations were repeated for values of T_{\max} ranging from 0.4–0.6°K. (For $T_{\max} < 0.4^\circ\text{K}$, not enough points were included in the least-squares fit, while for $T_{\max} > 0.6^\circ\text{K}$, data were drawn from regions where the power law is manifestly violated.) We found that, for the majority of the demagnetizations, n_{\min} fell between 2 and 4. Changes in the constant B when T_{\max} and n_{\min} were varied over their ranges were generally smaller than the errors associated with balancing the phase detector and reading the delay dial. Consequently, we somewhat arbitrarily set $n=3$, $T_{\max}=0.5^\circ\text{K}$ in our final calculations, and conclude that this choice introduces no significant bias into the results.

2. Absence of Dispersion at 0°K

Measurements of u_1 by other workers (see Sec. V for references) indicate that, above 1.2°K, the change in velocity over the frequency interval 0.2–5 Mc/sec does not exceed 0.2%. The dispersion calculated from the Khalatnikov-Chernikova theory¹⁰ for the range 1–12 Mc/sec is approximately 0.4 cm/sec at 1.2°K and

vanishes rapidly at higher temperatures. Since our measurements show that, within experimental error, $\tau_r(T)$ is the same at 1, 4, and 12 Mc/sec for $T > 1.2^\circ\text{K}$, it seems a safe conclusion that the low-temperature asymptotes of u_1 are equal at these frequencies within 0.2% (~ 50 cm/sec).

In deriving $u_1(T)$ from $\tau_r(T)$, we have used the same value of u_{10} at all three experimental frequencies, thereby making the implicit assumption that there is no dispersion at all at 0°K. This assumption is stronger than the facts warrant, and strictly speaking it is probably wrong. For sufficiently low temperatures, within the so-called collisionless regime where the period of the sound wave is very short compared with the average time between thermal-phonon collisions ($\omega\tau \gg 1$), it is thought that the wave itself can be regarded as a collection of low-frequency phonons. If we suppose that the acoustic and thermal phonons obey the same dispersion law,²⁸

$$\epsilon = \hbar\omega = pu_{10}(1 - \gamma p^2), \quad (6)$$

where $p = \hbar/\lambda \cong \hbar\omega/u_1$, then the acoustic-phonon velocity will be

$$u_1(\omega) = \partial\epsilon/\partial p \cong u_{10}\{1 - \gamma(\hbar\omega/u_{10})^2\}.$$

Using Landau and Khalatnikov's value $\gamma = 2.8 \times 10^{87}$ (g cm/sec)⁻², we find that the velocity difference for the frequency interval 1–12 Mc/sec is less than 10^{-5} cm/sec. Measurements would have to be extended to frequencies above 10^9 cps to exhibit dispersion of the order of 1 mm/sec. If the frequency dependence of the velocity of sound at 0°K is indeed as weak as this estimate suggests, the assumption $u_{10} = \text{constant}$ should have no important consequences in the analysis and interpretation of our data. The dispersion from 1–12 Mc/sec at 0°K would have to be of the order of 1 cm/sec to invalidate the comparison to be made in the paragraphs below.

3. Dispersion at $T > 0^\circ\text{K}$

(a) Comparison with the Theory of Khalatnikov and Chernikova

To emphasize the frequency dependence of the velocity we subtract the velocities at 1 Mc/sec from those at 4 and 12 Mc/sec and plot the differences against temperature (Fig. 5). The dispersion is greatest near 0.9°K, where the absorption is also maximum. A theory of sound propagation in liquid helium developed recently by Khalatnikov and Chernikova^{9,10} has been found to give a satisfactory account of the behavior of the absorption coefficient,¹¹ particularly in the vicinity of the peak and on its high-temperature side, in the so-called hydrodynamic region. We will show that the predictions of the theory concerning the frequency

²⁸ L. D. Landau and I. M. Khalatnikov, Zh. Eksperim. i Teor. Fiz. 19, 637 (1949); 19, 709 (1949).

dependence of the velocity are also compatible with our present results.

The Khalatnikov-Chernikova (KC) treatment follows the lines of the theory of transport phenomena in liquid helium first elaborated by Landau and Khalatnikov²⁸ and later developed extensively by Khalatnikov.^{29,30} Like the earlier work, it is based upon a detailed consideration of the possible interactions among the phonons and the rotons. In summary, it is found that the cross section for roton-roton scattering is sufficiently large so that the rotons may be considered to be in local thermodynamic equilibrium at temperatures above approximately 0.6°K and at the frequencies used in past experimental studies (<15 Mc/sec). Equilibrium with respect to energy and number density for the phonons travelling in a given direction is rapidly brought about by the elastic four-phonon process and by the inelastic five-phonon process, whose scattering cross sections are large for small-angle collisions. It is concluded that sound absorption and dispersion near 1°K arise principally from two relatively slow processes: (1) the scattering of phonons by rotons, which enables the phonon and roton gases to come into equilibrium with each other; and (2) the scattering of phonons by other phonons through large angles, which brings about an isotropic distribution of the phonons with respect to energy. Above 1.2°K, the five-phonon process also plays a role.

The following expressions yield the behavior of the absorption coefficient and the velocity of ordinary sound for the temperature region below approximately 1.2°K:

$$\alpha_1 = -\frac{1}{2} \frac{\omega \rho_{n \text{ ph}}}{c \rho} \text{Im}(\varphi), \quad (7)$$

$$u_1(\omega, T) = u_1(0, T) - \frac{1}{2} \frac{\rho_{n \text{ ph}}}{\rho} \text{Re}(\varphi), \quad (8)$$

$$\varphi = z_{\text{ph r}} - 3 \frac{u^2 \ln a + \{2u z_{\text{ph r}} + z_{\text{ph r}}^2 [1 - \beta(1 - z_{\text{ph r}})] + 3u^2(1 - z_{\text{ph ph}})\} \{-2 + (z_{\text{ph ph}} + z_{\text{ph ph}} - 1) \ln a\}}{2 + [1 - z_{\text{ph ph}} + (1 - \beta)(1 - z_{\text{ph r}})] \ln a + 3(1 - z_{\text{ph ph}})[1 - \beta(1 - z_{\text{ph r}})] [-2 + (z_{\text{ph r}} + z_{\text{ph ph}} - 1) \ln a]},$$

$$z_{\text{ph r}} = 1 - (i\omega\tau_{\text{ph r}})^{-1}, \quad z_{\text{ph ph}} = 1 - (i\omega\tau_{\text{ph ph}})^{-1}, \quad a = \frac{z_{\text{ph r}} + z_{\text{ph ph}}}{z_{\text{ph r}} + z_{\text{ph ph}} - 2}, \quad \beta = 3k_B T / \mu c,$$

$$\rho_{n \text{ ph}} / \rho = \frac{16\pi^5 k_B^4 T^4}{45h^3 \rho c^5}, \quad \tau_{\text{ph ph}}^{-1} = \frac{9(13!)k_B^9 (u+1)^4 T^9}{2^{13} h^7 \rho^2 c^{10}}, \quad \tau_{\text{ph r}}^{-1} = \frac{(2\pi)^{17/2} k_B^{9/2} \Gamma \rho_0^4 \mu^{1/2}}{h^7 \rho^2 c^5} T^{9/2} e^{-\Delta/k_B T},$$

$$\Gamma = \frac{2}{9} + \frac{1}{25} \left(\frac{p_0}{\mu c} \right) + \frac{2}{9} A \left(\frac{p_0}{\mu c} \right)^2 + A^2, \quad A = \left(\frac{\Delta}{p_0 c} \right) \left(\frac{\rho^2 \partial^2 \Delta}{\Delta \partial \rho^2} \right) + \left(\frac{p_0}{\mu c} \right) \left(\frac{\rho \partial p_0}{p_0 \partial \rho} \right)^2, \quad (9)$$

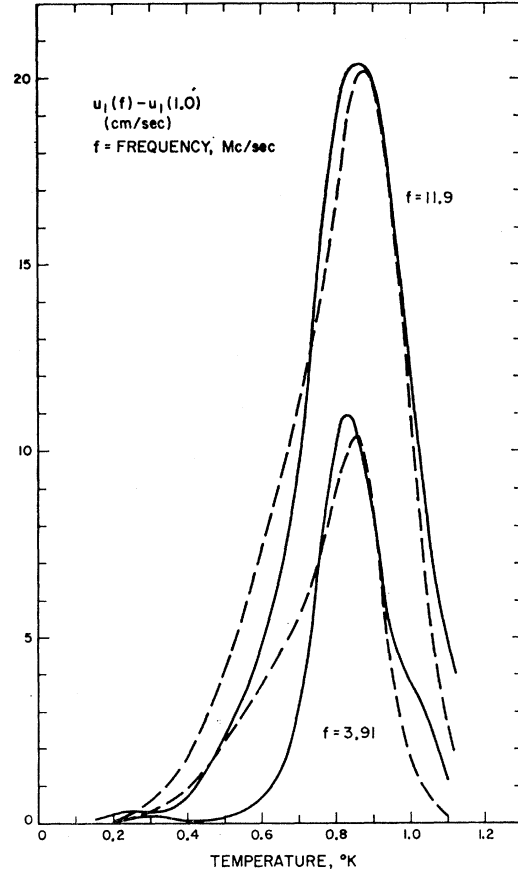


FIG. 5. Velocity difference over the frequency intervals 1.00–3.91 and 1.008–11.9 Mc/sec, plotted against temperature. Solid line represents smoothed experimental results; dashed line, dispersion evaluated from the Khalatnikov-Chernikova equations. Above 1°K, the errors in the delay measurement grow with increasing temperature, and the scatter in the velocity differences computed from our data becomes greater than the separation between the two experimental curves.

²⁹ I. M. Khalatnikov, Zh. Eksperim. i Teor. Fiz. 20, 243 (1950).

³⁰ I. M. Khalatnikov, Zh. Eksperim. i Teor. Fiz. 23, 8 (1952); 23, 21 (1952).

where c is the phonon velocity ($\cong u_{10}$), $u = (\rho/c)\partial c/\partial\rho$, ρ is the liquid density, and Δ , p_0 , and μ are Landau's roton parameters.

Equation (9) defining φ is valid only at temperatures for which five-phonon scattering is unimportant: $\tau_{3\rightarrow 2}/\tau_{\text{ph r}} \ll 1$. When allowance is made for this process, a very complicated set of equations results, and analytic expressions for the attenuation coefficient and velocity are given by KC only for frequencies sufficiently small that $\omega\tau_{\text{ph r}} \ll 1$:

$$\alpha_1 = \frac{\omega^2 \bar{\tau}_{\text{ph r}} \rho_{\text{ph}}}{c \rho} \left\{ \frac{2}{15} + \frac{(3u+1)^2}{6\tilde{\beta}} \right\}, \quad (10)$$

$$u_1(\omega, T) \cong u_1(0, T),$$

$$\bar{\tau}_{\text{ph r}}/\tau_{\text{ph r}} = 1 + \frac{27}{\pi^4} \left(\frac{\pi^4}{216} - 1 \right)^2 \bigg/ \left(\frac{\pi^4}{56 \times 216} + \frac{\tau_{\text{ph r}}}{\tau_{3\rightarrow 2}} \right), \quad (11)$$

$$\tilde{\beta}^{-1} = \left[\beta^{-1} + \left(\frac{27}{\pi^4} - \frac{1}{9} \right) \frac{\tau_{3\rightarrow 2}}{\tau_{\text{ph r}}} \right] \frac{\tau_{\text{ph r}}}{\bar{\tau}_{\text{ph r}}}, \quad (12)$$

$$\tau_{3\rightarrow 2}^{-1} = \frac{\Lambda c^3 T^9 \hbar^3}{24\pi\zeta(3)k_B^2} (\zeta(3) \cong 1.202).$$

The constant Λ characterizing the five-phonon process has to be evaluated by fitting the expression given for α_1 in Eq. (10) to experimental values of the attenuation coefficient.

According to KC, Eq. (10) is applicable for $T > 1.2^\circ\text{K}$. At 12 Mc/sec, $\omega\tau_{\text{ph r}} \cong 3 \times 10^{-2}$ at 1.2°K , so the condition $\omega\tau_{\text{ph r}} \ll 1$ will be satisfied at higher temperatures for all three of the frequencies used in our experiment. We expect no dispersion at such temperatures and we have observed none. However, $\tau_{3\rightarrow 2}/\tau_{\text{ph r}} \cong 7$ at 1.2°K . One therefore expects that five-phonon scattering will still be contributing to the absorption and the dispersion here and at lower temperatures, and it seems desirable somehow to make allowance for this process in evaluating Eq. (8) for the high-temperature side of the velocity maximum, where the dispersion is vanishing. To make approximate calculations for this region, for which Khalatnikov and Chernikova provide no explicit solution, we follow an interpolation procedure suggested by Hohenberg³¹ and substitute $\tilde{\beta}$ and $\bar{\tau}_{\text{ph r}}$, as defined by Eqs. (11) and (12), for β and $\tau_{\text{ph r}}$ wherever they appear in Eq. (9). To justify this step, we note that, according to KC, the low-frequency limit of Eq. (7) for α_1 for the temperature region $0.9^\circ\text{--}1.2^\circ\text{K}$ has the form

$$\alpha_1 = \frac{\omega^2 \tau_{\text{ph r}} \rho_{\text{ph}}}{c \rho} \left\{ \frac{2/15}{1 + \tau_{\text{ph r}}/\tau_{\text{ph ph}}} + \frac{(3u+1)^2}{6\beta} \right\}. \quad (13)$$

Since Eq. (10) was derived under less restrictive assumptions than Eq. (13), we might expect that the

low-frequency limit of the most general expression for α_1 near 1°K would more closely resemble (10) than (13). The substitutions indicated above thus naturally suggest themselves. When they are made, the attenuation and the velocity can be calculated each from a single expression over the entire temperature region of interest to us. We find that, from approximately $1\text{--}1.2^\circ\text{K}$, the velocity differences derived from Eq. (8) are in somewhat better agreement with our present measurements when Hohenberg's interpolation scheme is used than when it is not. It should be emphasized, however, that the approximation is useful only at frequencies for which $\omega\tau_{\text{ph r}} < 1$ at temperatures where $\tau_{\text{ph r}}/\tau_{\text{ph r}} < 1$, and will lose validity at higher frequencies. When $\tilde{\beta}$ and $\bar{\tau}_{\text{ph r}}$ are substituted for β and $\tau_{\text{ph r}}$ in Eq. (7), the peak attenuation decreases by 8% at 12 Mc/sec and by almost 25% at 723 Mc/sec. (The peak dispersion for the frequency interval $1\text{--}12$ Mc/sec decreases by only 3%.) Thus it appears that the solution of the equations given by Khalatnikov and Chernikova for the temperature region where the five-phonon process is important will have to be extended to cover the frequency range $\omega\tau_{\text{ph r}} \gtrsim 1$ before a completely satisfying comparison can be made with the recent attenuation measurements of Abraham, Eckstein, Ketterson, and Vignos³² at 30, 90, and 150 Mc/sec and of Woolf, Platzman, and Cohen³³ at 556 and 723 Mc/sec.

We have evaluated the differences $u_1(\omega_2, T) - u_1(\omega_1, T)$ from Eq. (8) with $c = u_{10} = 2.383 \times 10^4$ cm/sec, $\rho = 0.145$ g/cm³, $u = 2.64$,³⁴ $\Delta/k_B = 8.65$ K^o, $\mu = 1.06 \times 10^{-24}$ g, $p_0 = 2.02 \times 10^{-19}$ g/cm sec,³⁵ and $\Gamma = 2.6$. The last number is obtained if $A = -0.1$, as suggested by Khalatnikov and Chernikova⁹ after an analysis of neutron-scattering data. In place of their value $\Lambda = 3.4 \times 10^{43}$ we use $\Lambda = 2.7 \times 10^{43}$, which was obtained by fitting Eq. (10) to the attenuation data of Chase¹⁹ and of Dransfeld, Newell, and Wilks³⁶ from $1.15\text{--}1.8^\circ\text{K}$. (These measurements were chosen because they were made with variable ultrasonic path.)

The predicted velocity differences for the frequency intervals $1\text{--}4$ and $1\text{--}12$ Mc/sec are shown as broken lines in Fig. 5. It is apparent that the agreement between the experimental curves and those derived from the new theory is, on the whole, excellent. The heights and locations of the dispersion maxima are accounted for, as is the vanishing of the dispersion near 1.2°K . There are some discrepancies on the low-temperature side of the peak, but in view of the systematic errors discussed in an earlier section it is difficult to make a firm statement as to whether or not the disagreement is signif-

³² B. M. Abraham, Y. Eckstein, J. B. Ketterson, and J. H. Vignos, Phys. Rev. Letters **16**, 1039 (1966).

³³ M. A. Woolf, P. M. Platzman, and M. G. Cohen, Phys. Rev. Letters **17**, 294 (1966).

³⁴ K. R. Atkins and R. A. Stasior, Can. J. Phys. **31**, 1156 (1953).

³⁵ J. L. Yarnell, G. P. Arnold, P. J. Bendt, and E. C. Kerr, Phys. Rev. **113**, 1379 (1959).

³⁶ K. Dransfeld, J. A. Newell, and J. Wilks, Proc. Roy. Soc. (London) **A243**, 500 (1958).

³¹ P. C. Hohenberg (private communication).

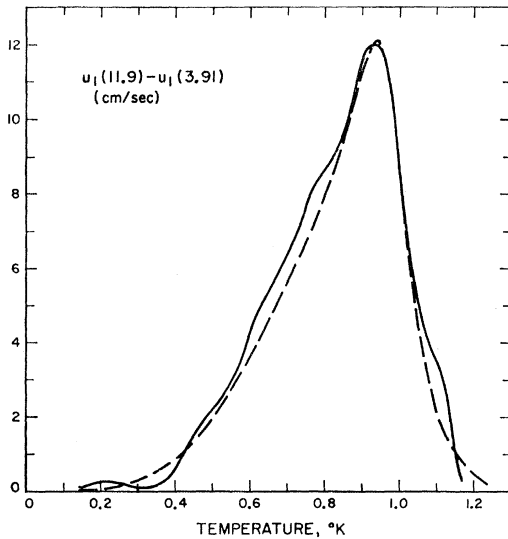


FIG. 6. Velocity difference over the frequency interval 3.91–11.9 Mc/sec, plotted against temperature. Solid line represents smoothed experimental results; dashed line, dispersion evaluated from the Khalatnikov-Chernikova equations.

icant. Since the results at all three frequencies were adjusted to coincide at 0°K, one expects that errors in the delay differences, such as those arising from standing waves in the delay line or from amplitude distortion, would increase with temperature, and therefore be less important below the dispersion peak than above. Nevertheless it can be seen that the velocity differences for the intervals 1–4 and 1–12 Mc/sec both lie below their corresponding theoretical curves by roughly equal amounts. To investigate the possibility that these discrepancies arise from systematic errors in the 1-Mc/sec results, we plot measured and predicted velocity differences for the frequency interval 4–12 Mc/sec in Fig. 6. Such good agreement as that now exhibited must be considered largely fortuitous, but it does suggest that what quantitative differences there are between the two sets of curves shown in Fig. 5 should not be emphasized. We conclude that the predictions of Khalatnikov and Chernikova's new theory are fully compatible with our measurements within the limits set by experimental errors.

It is particularly noteworthy that all but one of the parameters needed for the evaluation of the theoretical equations can be derived from other experiments. The single exception is Λ , and the process that makes the introduction of this constant necessary does not have a major influence on the behavior exhibited in Figs. 5 and 6. Khalatnikov's 1950 theory of sound propagation in liquid helium,²⁹ which invoked a physical model somewhat different from that of KC and required two adjustable constants, led to the prediction of the absorption maximum before it was observed¹⁹ and gave a good account of the temperature and pressure de-

pendence of the absorption coefficient above 0.8°K.^{19,36} We find that it also yields numerical values in satisfactory agreement with our present velocity measurements near the dispersion peak and above, but the agreement is poor below the peak.

(b) Comparison with Three-Phonon Theory

A number of authors in recent years³⁷ have attempted to show that the absorption of sound in liquid helium at low temperatures and high frequencies can be attributed to the direct absorption of an acoustic phonon by a thermal phonon: $\mathbf{p}_s + \mathbf{p}_{th} = \mathbf{p}'_{th}$. Khalatnikov and Chernikova do not consider this process; Landau and Khalatnikov²⁸ and Khalatnikov²⁹ explicitly ruled it out. In these treatments, liquid helium is regarded in first approximation as an assembly of thermal quanta, each with zero spectral width for given momentum. The interactions that broaden the energy levels and limit the lifetimes are introduced by perturbation theory, and it is found that the direct three-phonon process is prohibited because energy and momentum cannot be conserved simultaneously in the interaction of three "bare" phonons. The three-phonon theories start with the notion that the thermal phonon is in fact a quasiparticle with finite lifetime τ and spectral width $\delta\epsilon \sim \hbar/\tau$. In the interaction of two of these "dressed" or renormalized phonons with each other, there is a range of energy, for given total momentum of the colliding phonons, over which the process can take place. If the range exceeds the amount by which conservation of energy would be violated in a collision involving the three corresponding bare phonons, the process can occur with an appreciable probability. The condition that must be fulfilled is stated

$$1 < \omega\tau < \{3\gamma\langle p_{th}^2 \rangle\}^{-1}, \quad (14)$$

where γ is the phonon dispersion parameter defined in (6).

According to Leggett and ter Haar,³⁸ the two approaches mentioned above are equivalent; consequently before comparing our results with the predictions of the three-phonon theory, we should first determine whether or not these predictions are essentially different from those of Khalatnikov and Chernikova. We shall find that, in first order at least, they are not.

At temperatures and frequencies for which the inequality (14) is satisfied ($T \lesssim 0.4^\circ\text{K}$ at 12 Mc/sec), the KC expressions for the attenuation coefficient and velocity can be reduced to the simple forms

$$\alpha_1 = -\frac{3\omega}{4c} (u+1)^2 \frac{\rho_{nph}}{\rho} \tan^{-1}(2\omega\tau_{ph}), \quad (15)$$

³⁷ See Ref. 38 for a listing of the relevant papers.

³⁸ A. J. Leggett and D. ter Haar, Phys. Rev. **139**, A779 (1965).

$$\delta u_1(\omega, T) \equiv u_1(\omega, T) - u_1(0, T)$$

$$= -\frac{3}{8}(u+1)^2 c \frac{\rho_{n \text{ ph}}}{\rho} \ln(1+4\omega^2 \tau^2_{\text{ph ph}}). \quad (16)$$

The theory based upon the three-phonon process has apparently been carried furthest by Kwok, Martin, and Miller,³⁹ and by Pethick and ter Haar.¹² The latter authors give expressions for $\delta u_1(\omega, T)$ as well as for α_1 ⁴⁰:

$$\alpha_1 = -\frac{3}{4} \frac{\omega}{c} (u+1)^2 \frac{\rho_{n \text{ ph}}}{\rho} \times \{ \tan^{-1}(2\omega\tau) - \tan^{-1}(3\gamma\omega\tau \langle p_{\text{th}}^2 \rangle) \}, \quad (17)$$

$$\delta u_1(\omega, T) = -\frac{3}{8}(u+1)^2 c \frac{\rho_{n \text{ ph}}}{\rho} \times \ln \left\{ \frac{1+4\omega^2 \tau^2}{1+\{3\gamma\omega\tau \langle p_{\text{th}}^2 \rangle\}^2} \right\}. \quad (18)$$

When the inequality (14) is satisfied, these equations are the same as (15) and (16). At lower temperatures, where

$$\omega\tau > \{3\gamma \langle p_{\text{th}}^2 \rangle\}^{-1} > 1, \quad (19)$$

the spectral width of the thermal phonons grows small and the contribution of the direct three-phonon process to the absorption vanishes. To find the limiting forms taken by Eqs. (17) and (18) in this region, we expand the arctangent functions about $\pi/2$ and make

³⁹ P. C. Kwok, P. C. Martin, and P. B. Miller, *Solid State Commun.* **3**, 181 (1965).

⁴⁰ In writing Eq. (17) we have dropped a factor $\pi/2$ that appears erroneously in Eq. (5.6) of Ref. 12 [C. J. Pethick (private communication)].

the approximations dictated by (19):

$$\alpha_1 = -\frac{3}{4}(u+1)^2 c \frac{\rho_{n \text{ ph}}}{\rho} \{3\gamma c \tau \langle p_{\text{th}}^2 \rangle\}^{-1},$$

$$\delta u_1(\omega, T) = -\frac{3}{4}(u+1)^2 c \frac{\rho_{n \text{ ph}}}{\rho} \ln \left(\frac{3}{2} \gamma \langle p_{\text{th}}^2 \rangle \right).$$

For the same temperature region, Khalatnikov and Chernikova give equations almost identical with these, the only difference being that the factor $(2\pi k_B T/c)^2 (5/6)$ appears in place of $\langle p_{\text{th}}^2 \rangle$, while Pethick and ter Haar have set $\langle p_{\text{th}}^2 \rangle = (3k_B T/c)^2$. Thus no further comparison between Eq. (18) and our present results is necessary. The fact is that our measurements do not extend to high enough frequencies or low enough temperatures to provide an adequate test of Eq. (18) alone.⁴¹ In its present form, the three-phonon theory ignores rotons, and consequently becomes invalid above approximately 0.6°K. The more complete KC theory, which is not limited to the phonon gas, is applicable over the entire temperature region covered in our measurements.

ACKNOWLEDGMENTS

We are indebted to T. Oversluizen for technical assistance and to R. Oder, J. Rosenshein, A. Thiele, and R. Williamson for help given during the experimental runs. We have benefited from conversations with many colleagues; in particular we wish to acknowledge a helpful effort by M. M. Saffren to increase our understanding of certain aspects of the three-phonon theory, and an instructive remark by T. M. Sanders, Jr., concerning dispersion at 0°K.

⁴¹ The recent measurements of Abraham *et al.* (Ref. 32) at 30, 90, and 150 Mc/sec at temperatures extending down to 0.12°K provide much more direct support for Eq. (17) [and thus for Eq. (15) as well] for the regime $\omega\tau \gg 1$.